Journal of Atmospheric and Solar-Terrestrial Physics 163 (2017) 114–119

Contents lists available at ScienceDirect

Journal of Atmospheric and Solar-Terrestrial Physics

journal homepage: www.elsevier.com/locate/jastp

Earth's magnetic field effect on MUF calculation and consequences for hmF2 trend estimates

Ana G. Elias [a,b,*], Bruno S. Zossi [a,b], YigitErdal Yiğit [c], Zenon Saavedra [b,d], Blas F. de Haro Barbas [a]

[a] Laboratorio de Fisica de la Atmosfera, Departamento de Fisica, Facultad de Ciencias Exactas y Tecnología, Universidad Nacional de Tucuman, Av. Independencia 1800, 4000 Tucuman, Argentina
[b] Consejo Nacional de Investigaciones Cientificas y Tecnicas, CONICET, Argentina
[c] Department of Physics and Astronomy, George Mason University, 4400 University Drive, Fairfax, VA 22030, USA
[d] Laboratorio de Telecomunicaciones, Departamento de Electricidad, Electronica y Computacion, Facultad de Ciencias Exactas y Tecnologia, Universidad Nacional de Tucuman, Av. Independencia 1800, 4000 Tucuman, Argentina

ARTICLE INFO

Keywords:
Geomagnetic field
Long-term trends
Ionosphere
M(3000)F2
Ionospheric refractive index

ABSTRACT

Knowledge of the state of the upper atmosphere, and in particular of the ionosphere, is essential in several applications such as systems used in radio frequency communications, satellite positioning and navigation. In general, these systems depend on the state and evolution of the ionosphere. In all applications involving the ionosphere an essential task is to determine the path and modifications of ray propagation through the ionospheric plasma. The ionospheric refractive index and the maximum usable frequency (MUF) that can be received over a given distance are some key parameters that are crucial for such technological applications. However, currently the representation of these parameters are in general simplified, neglecting the effects of Earth's magnetic field. The value of M(3000)F2, related to the MUF that can be received over 3000 km is routinely scaled from ionograms using a technique which also neglects the geomagnetic field effects assuming a standard simplified propagation model. M(3000)F2 is expected to be affected by a systematic trend linked to the secular variations of Earth's magnetic field. On the other hand, among the upper atmospheric effects expected from increasing greenhouse gases concentration is the lowering of the F2-layer peak density height, hmF2. This ionospheric parameter is usually estimated using the M(3000)F2 factor, so it would also carry this "systematic trend". In this study, the geomagnetic field effect on MUF estimations is analyzed as well as its impact on hmF2 long-term trend estimations. We find that M(3000)F2 increases when the geomagnetic field is included in its calculation, and hence hmF2, estimated using existing methods involving no magnetic field for M(3000)F2 scaling, would present a weak but steady trend linked to these variations which would increase or compensate the few kilometers decrease (~2 km per decade) expected from greenhouse gases effect.

1. Introduction

The ionosphere is the plasma region of the upper atmosphere that is coupled to meteorological processes from below (Yiğit and Medvedev, 2015) and to space weather effects from above (Yiğit et al., 2016). Ionospheric measurements began in the early 1900s with a high-frequency radar known as ionosonde, which sends vertically short pulses of high-frequency electromagnetic waves. At a certain height these waves are reflected back toward the ground and the ionosonde records the time delay, T, between the transmitted and the received signal (Reinisch et al., 1998). Assuming the signal propagation is at the speed of light in vacuum, c, for the whole path, a virtual height, h′, also called equivalent (or apparent) height, can be estimated from

$$h' = \frac{c}{2}T. \quad (1)$$

The virtual height at a given frequency is then the distance that the electromagnetic wave would have traveled in half the elapsed time T at the speed of light. Since electromagnetic waves within the ionosphere travel more slowly than c, i.e., with group velocity v_g<c, the actual height

* Corresponding author at: Laboratorio de Fisica de la Atmosfera, Departamento de Fisica, Facultad de Ciencias Exactas y Tecnología, Universidad Nacional de Tucuman, Av. Independencia 1800, 4000 Tucuman, Argentina.
E-mail addresses: aelias@herrera.unt.edu.ar (A.G. Elias), brunozossi@hotmail.com (B.S. Zossi), eyigit@gmu.edu (E. Yiğit), zsaavedra@herrera.unt.edu.ar (Z. Saavedra), blasdeharo2000@yahoo.com.ar (B.F. de Haro Barbas).

https://doi.org/10.1016/j.jastp.2017.03.004
Received 2 December 2016; Received in revised form 13 February 2017; Accepted 9 March 2017
Available online 11 March 2017

of a reflecting reference layer is smaller than the deduced h′.

Ionograms are produced by varying the wave frequency and then plotting h′ in terms of frequency.

Obtaining the true height electron density profile from ionogram data is a complex procedure for which several methods have been developed (Scotto et al., 2012). In particular, the peak height of the profile at which the maximum electron density occurs, hmF2, can be estimated in a simple way using its inverse relation to M(3000)F2 factor (Shimazaki, 1955; Bilitza et al., 1979; Dudeney, 1983), which corresponds to the maximum usable frequency (MUF) at which a radio wave can propagate from a given point over a distance of 3000 km divided by foF2.

The most widely used formula is given by Shimazaki (1955) assuming an F2 layer with no underlying ionization, and neglecting the geomagnetic field, that is

$$hmF2 = \frac{1490}{M(3000)F2} - 176 \tag{2}$$

A correction ΔM was introduced later to consider a more realistic ionosphere so that Eq. (2) becomes

$$hmF2 = \frac{1490}{M(3000)F2 + \Delta M} - 176 \tag{3}$$

Bradley and Dudeney (1973) took into account the underlying ionization and obtained for ΔM the following expression

$$\Delta M = \frac{0.18}{\frac{foF2}{foE} - 1.4} \tag{4}$$

Bilitza et al. (1979) considered in addition the solar activity level through the 12-month running mean sunspot number, R_{12}, and Earth's magnetic field including in the formula the dip latitude, ϕ. ΔM then yields

$$\Delta M = \frac{f_1 \times f_2}{\frac{foF2}{foE} - f_3} + f_4 \tag{5}$$

where

$$f_1 = 0.00232 \quad R_{12} + 0.222 \tag{6}$$

$$f_2 = 1 - \frac{R_{12}}{150} e^{-\varnothing^2/1600} \tag{7}$$

$$f_3 = 1.2 - 0.0116 \quad e^{R_{12}/4.84} \tag{8}$$

$$f_4 = 0.096 \frac{R_{12} - 25}{150} \tag{9}$$

The increasing interest in long-term trends in the upper atmosphere in the context of climate change, mainly attributed to the increasing greenhouse gases concentration, brought the search of long ionospheric data series (encompassing several decades), specially of hmF2. In fact, according to earlier theoretical models (Roble and Dickinson 1989; Rishbeth 1990) the increased concentration of greenhouse gases would induce a cooling in the thermosphere, together with a decrease in air density and a contraction of the upper atmosphere, with a consequent decrease of ionospheric layers. For a hypothetical scenario of doubling of CO_2 a cooling of 30–40 K in the thermosphere was modeled and an hmF2 decrease of 15–20 km. Observations have supported this hypothesis for the actual changes in CO_2 (Qian et al., 2011; Zhang et al., 2011; Lastovicka et al., 2014) but have also suggested that an increase in CO_2 does not completely account for the observed thermospheric temperature trend (Zhang et al., 2016).

In order to assess long-term trends in hmF2, or in any other ionospheric parameter, the solar activity effect must be excluded first since solar variations have a significant impact at F2 region altitudes especially via the associated variability in the direct solar insolation and high-latitude energy and momentum inputs. As the solar activity has a prominent ~11 year periodicity, and considering that trends are more reliable for longer data intervals (Mielich and Bremer, 2013), at least 2 to 3 decades of data are needed in order to obtain statistically significant results. In fact, most of the publications on hmF2 trend analysis use the longer data series available in order to obtain reliable results, with most of the records dating back to the International Geophysical Year 1957, and some with the earliest records since the 1940s (Ulich and Turunen, 1997; Upadhyay and Mahajan, 1998; Mikhailov and Marin, 2001). This requirement on data series length led researchers to use ionospheric characteristics scaled manually from film or paper ionograms made by the ionosondes that preceded the modern digital ionosondes (McNamara, 2008), with the only options for hmF2 estimation through M(3000)F2 or hpF2 that is the virtual height at a frequency equal to 0.834 foF2, which can be used as a substitute for hmF2 (Zolessi and Cander, 2014).

The hmF2 data series that have been analyzed in most of the publications until now, are obtained through the Shimazaki (1955) (Eq. (2)) or Bradeley and Dudeney (1973) formula (Eq. (4)) which uses M(3000)F2 without any consideration of Earth's magnetic field and its variations. Being aware of this limitation, apart from the necessity of a special quality control of the data when dealing with historical data sets stressed by many authors and especially in the work by McNamara (2008), we want here to emphasize the importance of considering the effect of geomagnetic field secular variations on an ionospheric characteristic such as M(3000)F2 which is widely used to detect ionospheric trends.

This factor is obtained manually using a transmission-curve based on the propagation of radio signals in the ionosphere neglecting Earth's magnetic field. Current studies assume that the error associated with this approximation is insignificant compared to other error sources such as the assumption of geographic uniformity of the ionosphere over the transmission path. Assuming a constant geomagnetic field this assumption would not lead to an error in hmF2 trend estimation. It consists at most in a constant systematic error for not taking into account a factor in M(3000)F2 estimation that affects absolute values but do not affect slope assessments in linear trend analysis. However, the terrestrial magnetic field varies, with the most drastic change being a polarity reversal that takes place on average every ~200 000 years (Glassmeier et al., 2009). This means that the error introduced in hmF2 estimation using M(3000)F2, varies accordingly. Since the expected hmF2 trends as a consequence of greenhouse effect are less than 1%/year, the "trending" error associated with ignoring the magnetic field effects could completely screen it.

There is in addition the error associated with the hmF2 calculation. A thorough and deep analysis of the accuracy of hmF2 formulas using M(3000)F2 has been performed in the work by McNamara (2008). Considering that the uncertainty in scaled values of M(3000)F2 is ±0.05 MHz plus a random component raising it to 0.1, a ~15 km error in hmF2 results using the Shimazaki formula, for example. As stated in the work by McNamara (2008), if errors are random, they should be overcome using hmF2 monthly medians derived using the corresponding formula.

In the present work the terrestrial magnetic field effects on M(3000)F2 and the error introduced in hmF2 obtained through formulas in terms of M(3000)F2 are analyzed. Possible hmF2 trends induced by geomagnetic field secular variations on M(3000)F2 are compared to trend values expected from the long-term thermosphere cooling linked presumably to increasing greenhouse gases concentration.

Section 2 describes how M(3000)F2 is obtained through ionograms manual scaling. In Section 3 the effect of considering Earth's magnetic field is analyzed together with the consequences of secular variations, followed by Section 4 where Bilitza's formula is analyzed for a varying magnetic field. Finally, discussion and conclusions are presented in Section 5.

2. M(3000)F2 estimated from ionograms

The propagation factor M(3000)F2 is routinely scaled from ionograms by a standard graphical method (Piggott and Rawer, 1978). This method employs what is called a transmission curve (Smith, 1939), which gives the ratio of the equivalent vertical frequency and oblique incidence frequency of 3000 km distance range, both reflected from a given virtual height. The curve is constructed assuming a standard simplified propagation model. Values of this ratio in terms of virtual height to construct the transmission curve are given in a table in the Handbook of Ionogram Interpretation and Reduction by Piggott and Rawer, page 23) (1978). If the ionogram has a logarithmic frequency scale, the transmission curve, drawn in a transparent slider, is moved along the frequency axis until it touches the ordinary ray trace. The abscissa value given on the slider at foF2 is M(3000)F2. If the ionogram frequency scale is not logarithmic a set of standard curves is prepared from the standard transmission curve, each one corresponding to a given MUF value. The curve which touches the trace gives the MUF, and M(3000)F2 is obtained dividing this value in foF2.

The transmission curve calculation is based on two theorems that neglect Earth's magnetic field assuming a refractive index μ given by

$$\mu = \sqrt{1 - \frac{f_o^2}{f^2}} \tag{10}$$

where f is the frequency of the transmitted wave and f_o is the plasma frequency, given by

$$f_o = \sqrt{\frac{Ne^2}{\pi m}} \tag{11}$$

where N is the electron number density, e is the electron charge, and m is the electron mass. The first is Breit and Tuve's theorem which states that the equivalent path P′ between transmitter and receiver separated by a certain distance D is given by the length of the equivalent triangle with height h′, where h′ is the equivalent or virtual height where the wave would have been reflected assuming no refraction during its entire path. The second is Martyn's theorem stating that the virtual height of reflection of an obliquely incident wave is the same as that of the equivalent vertical wave. That is, the virtual height measured at vertical incidence, h′, for a frequency f_o is the same as the height of the equivalent triangular path of distance range D for an oblique higher frequency $f=f_o$ sec ϕ_1, where ϕ_1 is the angle between the ray entering the ionosphere through its lower boundary and the corresponding normal. To determine h′ and f corresponding to this transmission, we need to solve the vertical incidence equation $h' = h'(f_o)$ that is the ionogram profile, and the transmission equation $f_o = f/\sec\phi_1$, where ϕ_1 is determined from the height equivalence between a vertical and oblique path and the geometry of the path.

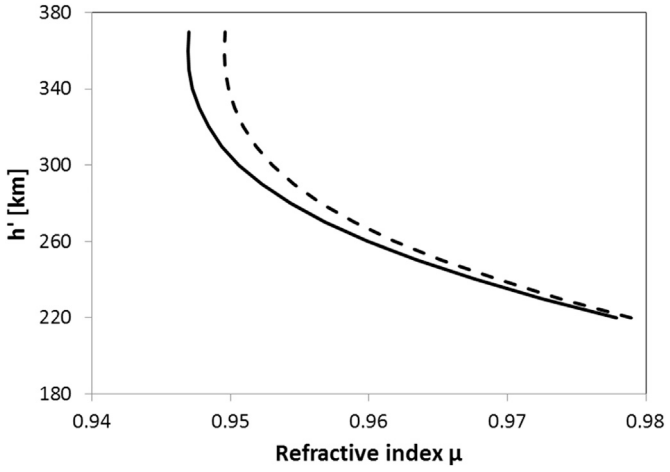

Fig. 1. Refractive index, μ, estimated with Eq. (10) neglecting B (solid line) and using Eq. (13) for B=50,000 nT and θ=0° (dashed line).

The solution is obtained graphically from the intersection between the frequency-virtual height curve of the ionogram and a family of curves of h′ in terms of f_o obtained from the transmission equation for different values of f and D, called transmission curves. The intersection with one of them for given f and D, gives the height of the equivalent triangular path for transmission for f over distance D, and also f for that path. The transmission curve is then a plot of f_o against h′, as the ionogram, but fulfilling the equation $f_o = f/\sec\phi_1$. If the frequencies are plotted logarithmically the transmission curve becomes a logarithmic curve of $1/\sec\phi_1$, which can be used for any f′ and D. The MUF over a given distance is the highest frequency for which the two curves have a point in common, that is when the transmission curve becomes tangent to the ionogram profile. The frequency corresponding to $\sec\phi_1 = 1$ is then the MUF for that distance.

Considering Earth's curvature, ϕ_1 is connected to D and h′ through the following equation

$$\tan\phi_1 = \frac{\sin\frac{D}{2R}}{\frac{h'}{R} + 1 - \cos\frac{D}{2R}} \tag{12}$$

where R is Earth's radius (6378 km).

To consider the curvature of the ionosphere, due to the complexity of the theoretical treatment (Davies, 1959), a factor k=1.115 is used, so finally M(3000)F2 results

$$M(3000)F2 = \frac{MUF(3000)}{foF2} = k\sec\phi_1 \tag{13}$$

The deduction of Eq. (13) assumes the absence of the geomagnetic field. This is clear from the refractive index given by Eq. (10) which is the result of the more general Appleton-Hartree equation neglecting collision. In the presence of a magnetic field B, μ would be given by (Ratcliffe, 1962)

$$\mu = \sqrt{1 - \frac{f_o^2}{f^2 - \frac{f^2 f_{BT}^2}{2\left(f^2 - f_0^2\right)} \pm \sqrt{\frac{f^2 f_{BT}^2}{2\left(f^2 - f_0^2\right)} + f^2 f_{BL}^2}}} \tag{13}$$

where

$$f_{BT} = f_B \sin\theta = \frac{eB}{2\pi mc}\sin\theta \tag{14}$$

and

$$f_{BL} = f_B \cos\theta = \frac{eB}{2\pi mc}\cos\theta \tag{15}$$

where f_B is the gyro-frequency, θ is the angle between the direction of the wave normal and B, T stands for transverse and L for longitudinal. The upper sign in the denominator of Eq. (13) refers to the ordinary component (o-component) and the lower sign to the extraordinary (x-component).

Breit and Tuve's and Martyn's theorems are no longer valid if B is taken into account in the wave propagation process; and with μ given now by Eq. (13) there is no simple relation between the quantities for vertical and oblique rays.

Among the first treatments of this problem, Smith (1939) gives an example of a transmission curve including B at the level of reflection showing clearly that a different curve should be considered. Haselgrove (1957) analyzed changes in both theorems concluding that Martyn's theorem is more inaccurate than Breit and Tuve's theorem. With a computer ray-tracing algorithm using the refractive index given by Eq.

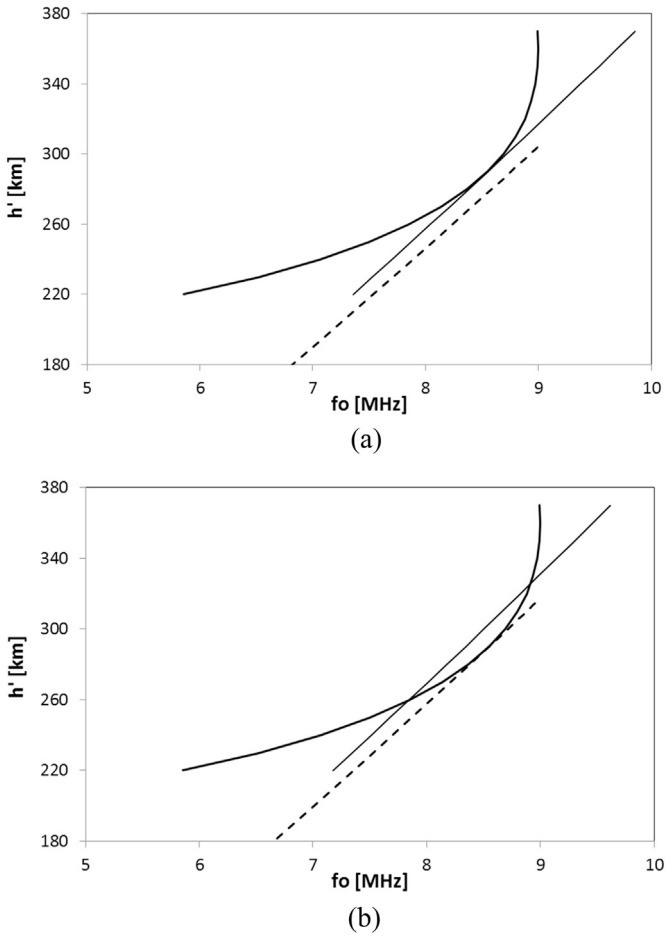

Fig. 2. Idealized h′(f_o) for a parabolic F2 layer (enhanced line) and transmission curves considering B=0 (solid line) and B=50,000 nT (dashed line), obtained for (a) f=MUF(3000)=28.6 MHz, which is the oblique frequency needed to obtain a transmission curve with B=0 tangent to the f_o profile, and (b) f=MUF(3000)=27.9 MHz, which is the oblique frequency needed to obtain a transmission curve with B=50,000 nT tangent to the f_o profile.

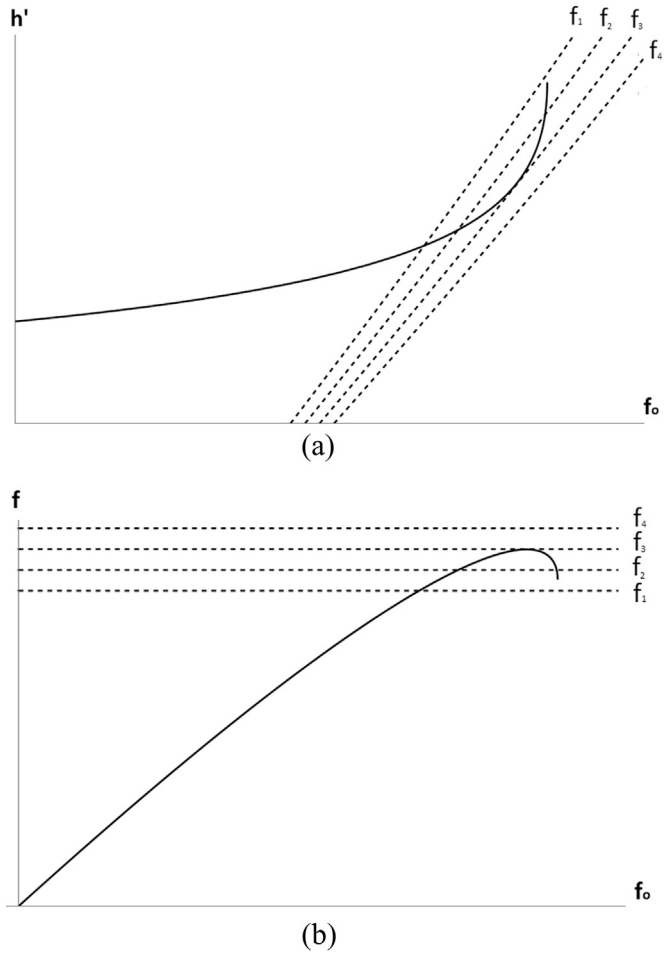

Fig. 3. (a) Scheme of a parabolic h′(f_o) profile (solid line) and transmission curves for different oblique frequencies (f) values (dotted line). (b) f in terms of f_o obtained from matching h′(f_o) and transmission curves for different f values.

(13) the errors were calculated for North-South transmission of the ordinary ray for a parabolic ionospheric layer and flat Earth. MUF values obtained were lower than predicted using Eq. (10). Davies (1959), after observing that direct MUF measurements were higher than those obtained using transmission curves, and that equivalent heights calculated including B are greater than neglecting this field, concludes that transmission curves should be different than the f/sec ϕ_1 plot and would depend on location.

Later Kopka and Möller (1968) resumed considering the effect of Earth's magnetic field on MUF calculating a correction term for the use of transmission curves.

3. Earth's magnetic field variation effect on M(3000)F2 from transmission curves

From Eq. (13) implies that inclusion of B with θ different from 90° result in μ increase. In Fig. 1 solid curve shows μ estimate using Eq. (10), that is neglecting B, and the dashed curve presents the results using Eq. (13) for B=50000 nT and θ=0 which corresponds approximately to the greatest B value at the F layer level and a longitudinal propagation. To obtain a simple estimation of this effect on M(3000)F2 when it is obtained using the transmission curve method, we make the following assumptions:

* ionogram h′(f_o) profile given by a parabolic F layer

* transmission equation still given by f_o=f/sec ϕ_1

*ϕ_1 at the reflection height satisfies μ=sin ϕ_1, with μ given by Eq. (13) instead of (10), that is

$$\sqrt{1-\frac{f_o^2}{f^2-\frac{f^2f_T^2}{2\left(f^2-f_0^2\right)}\ \pm\ \sqrt{\frac{f^2f_T^2}{2\left(f^2-f_0^2\right)}+f^2f_T^2}}}=\sin\left[tg^{-1}\left(\frac{\sin\frac{D}{2R}}{\frac{h'}{R}+1-\cos\frac{D}{2R}}\right)\right] \tag{16}$$

Transmission curves are obtained by solving Eq. (16) for h′ setting D=3000 km and given B and θ values. h′ is then a function of f_o and f only, and transmission curves are drawn as the corresponding set of (f_o, h′) for different f values.

Fig. 2 shows as an example an ionogram with foF2=9 MHz and h′F2=360 km and the transmission curves that correspond to h′ in terms of f_o obtained for both cases, B=0 and B‡0. In the first case, the transmission curve is estimated from f_o=f/sec ϕ_1, where ϕ_1 in terms of h′ is assessed using Eq. (2). In the second case, the same curve is calculated from Eq. (16) considering B=50,000 nT, that is approximately the maximum field value at the peak ionospheric height level, and θ=0.

To calculate the f value for which the transmission curve becomes tangent to h′(f_o) analytically, we match both equations and equate to zero the first derivative. Fig. 3 show schematically f in terms of f_o where it can be noticed the condition for one solution.

When B is neglected, the transmission curve becomes tangent to h′(f_o) for f=28.6 MHz, which corresponds to M(3000)F2=3.18 and hmF2=292.9 km according to Shimazaki (1955) formula. In the case of

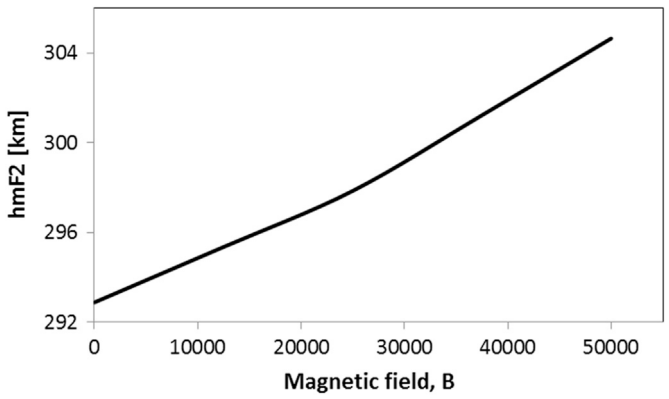

Fig. 4. hmF2 in terms of the Earth's magnetic field, B [nT], through M(3000)F2 estimated with the value of f for which the transmission curve becomes tangent to $h'(f_o)$ (idealized profile of Fig. 2 for a parabolic F2 layer).

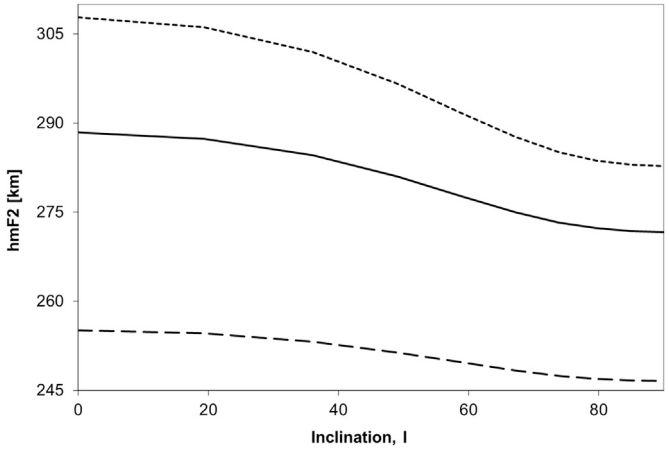

Fig. 5. Ionospheric electron density peak height, hmF2, calculated with Eq. (3) and M(3000)F2 correction factor, ΔM, given by Eq. (5), in terms of inclination, I. foE, foF2 obtained from IRI2012 for January, 12LT, 50°N, 40°E, for three different solar activity levels: Rz=50 (dashed line), 100 (solid line) and 150 (dotted line).

B=50,000 nT, the transmission curve becomes tangent to $h'(f_o)$ for f=27.9 MHz that is M(3000)F2=3.10 and hmF2=304.6 km. For a 50% decrease in B for example, the transmission curve becomes tangent to $h'(f_o)$ for f=28.3 MHz that corresponds now to M(3000)F2=3.14 and hmF2=297.9 km, that is 7 km lower. For a change in θ from 0 to 45° for example while keeping B=50,000 nT, f becomes 28.1 MHz, M(3000)F2=3.12 and hmF2=301.2 km, that is ~3 km lower. It should be noted that for higher hmF2 values the height difference between different B or θ conditions also increases. To have a clear idea of this situation, Fig. 4 shows hmF2 variation in terms of B in the range 0 – 50,000 nT through its effect on M(3000)F2 for ionospheric conditions considered in Fig. 2.

4. Earth's magnetic field variation effect on Bilitza's M(3000)F2 formula

The correction factor ΔM given by Eq. (5) (Bilitza et al., 1979) depends on magnetic inclination I through the dip latitude ϕ where $tg(\phi)=\frac{1}{2}\,tg(I)$, but not on the magnetic field intensity. Since I is changing with the geomagnetic field secular variations, hmF2 calculated with this ΔM in Eq. (3) will present a secular variation at a given location linked to the corresponding I variation.

Fig. 5 shows hmF2 variation for a representative location (50°N, 40°E) as a function of I, using Bilitza et al. (1979) formula, for different solar activity levels. I variation was forced through its entire range of values to make more noticeable hmF2 variation. The hmF2 absolute difference is bigger for higher Rz, that is for higher hmF2 values, as was noticed in the previous M(3000)F2 analysis. Also, for an I decrease, which would correspond to a θ increase, lower hmF2 values are obtained.

5. Discussion and conclusions

Trends in the upper and middle atmosphere has become a main subject since the beginning of the 1990's as a consequence of the increasing interest in global changes especially due to increasing greenhouse gases concentration, and several papers have been published since then on this topic (see Lastovicka et al. (2012) for a comprehensive review and references therein). A better estimation and prediction of thermospheric trends imposes a challenge from a fundamental science point of view as well as from a technological perspective as the morphology of the thermospheric temperature and density and the coexisting ionosphere are crucial for satellite mission planning and the associated life span.

Three key concepts should be highlighted: (1) secular changes in magnetic field can change the morphology of the ionosphere (including hmF2) due to inherent physical and chemical processes; (2) there are long-term changes not directly associated with Earth's magnetic field; and (3) measurement error and its long-term change due to ignoring Earth's magnetic field (and its secular change) in the routine hmF2 estimation. The true hmF2 will not change because of with and without considering magnetic field.

In this study, we have analyzed the significance of the terrestrial magnetic field effects on deducing the true height of an ionospheric layer, hmF2. When B is taken into account in M(3000)F2 calculation, the latter is always smaller than the value assessed neglecting B, so hmF2 results higher in as much as 10 km. In addition, a decrease in B would induce an increase in M(3000)F2 with a consequent decrease in hmF2 linked to this solely effect. Variations in the magnetic field inclination also affect M(3000)F2 assessment. This last case is also clearly evident in Bilitza's formula for ΔM.

Hence, the most pressing question that bares in mind is: What are the implications of the dependence of M(3000)F2 on Earth's magnetic field for the long-term trend analysis of hmF2?

Assume an hmF2 time series spanning several decades during which, together with the increase in greenhouse gases concentration, a net B decrease took place. Ideally, hmF2 determined without including B-effects in M(3000)F2 estimation, apart from the strong seasonal and solar activity effects, it should not present any other variation except a lowering according to the cooling effect expected at this atmospheric level. However, if B is included in the calculation of hmF2 a natural lowering should be obtained as a consequence of M(3000)F2 increase due solely to correctly accounting for the magnetic field without any consideration of greenhouse cooling.

Another point of consideration would be if hmF2 record consists in a mix of manually scaled values using M(3000)F2 at the beginning of the period analyzed plus autoscaled values at the end. hmF2 time series would consist of lower than real height values at the beginning followed by real heights towards the end. This would imply weaker than actual downward hmF2 trends.

Regarding Bilitza's formula, Ulich and Turunen (1997) and Bremer (1992) already used it for hmF2 trend estimations but they keep the inclination constant for the locations analyzed.

Even though the magnetic field introduces corrections to the transmission curves that may be of minor importance compared for example to other assumptions such as the geographic uniformity of the ionosphere over the transmission path, it could be comparable to the greenhouse gas effect for some locations and conditions, taking into account that the geomagnetic field effect on radio transmission varies with the length, direction and geographic location of the transmission path due to ionospheric anisotropy caused by this field.

Acknowledgments

This work was supported by Project PIUNT E541.

References

Bilitza, D., Sheikh, N.M., Eyfrig, R., 1979. A global model for the height of the F2-peak using M3000 values from CCIR. Telecommun. J. 46, 549–553.

Bradley, P., Dudeney, J.R., 1973. A simple model of the vertical distribution of electron, concentration in the ionosphere. J. Atmos. Terr. Phys. 35, 2131–2146.

Davies, K., 1959. The effect of the earth's magnetic field on m.u.f. calculations. J. Atmos. Terr. Phys. 16, 187–189.

Dudeney, J.R., 1983. The accuracy of simple methods for determining the height of the maximum electron concentration of the F2-layer from scaled ionospheric characteristics. J. Atmos. Terr. Phys. 45, 629–640.

Glassmeier, K.H., Soffel, H., Negendank, J.F.W., 2009. Geomagnetic Field Variations. Springer Verlag, Berlin.

Haselgrove, J., 1957. Oblique Ray Paths in the Ionosphere. Proceedings Phys. Soc. B 70, 653-662.

Kopka, H., Möller, H.G., 1968. MUF calculations including the effect of the earth's magnetic field. Radio Sci. 3, 53–56.

Lastovicka, J., Solomon, S.C., Qian, L., 2012. Trends in the neutral and ionized upper atmosphere. Space Sci. Rev. 168, 113–145.

Lastovicka, J., Beig, G., Marsh, D.R., 2014. Response of the mesosphere-thermosphere-ionosphere system to global change - CAWSES-II contribution. Prog. Earth Planet. Sci. 1, 1–21.

McNamara, L.F., 2008. Accuracy of models of hmF2 used for long-term trend analyses. Radio Sci. 43, RS2002. http://dx.doi.org/10.1029/2007RS003740.

Mikhailov, A.V., Marin, D., 2001. An interpretation of the foF2 and hmF2 long-term trends in the framework of the geomagnetic control concept. Ann. Geophys. 19, 733–748.

Mielich, J., Bremer, J., 2013. Long-term trends in the ionospheric F2 region with different solar activity indices. Ann. Geophys. 31, 291–303.

Piggott, W.R., Rawer, K., 1978. Report UAG-23A Handbook of Ionogram Interpretation and Reduction, Second ed. World Data Center A for Solar-Terrestrial Physics, NOAA, Boulder, Colorado, USA.

Qian, L., Laštovicka, J., Roble, R.G., Solomon, S.C., 2011. Progress in observations and simulations of global change in the upper atmosphere. J. Geophys. Res. 116, A00H03. http://dx.doi.org/10.1029/2010JA016317.

Ratcliffe, J.A., 1962. The Magneto-ionic theory and its applications to the ionosphere. Cambridge University Press, London, UK.

Reinisch, B., Scali, J., Haines, D., 1998. Ionospheric drift measurements with ionosondes. Ann. Geophys. 41 (5–6) http://dx.doi.org/10.4401/ag-3812.

Rishbeth, H., 1990. A greenhouse effect in the ionosphere? Planet. Space Sci. 38, 945–948.

Roble, R.G., Dickinson, R.E., 1989. How will changes in carbon dioxide and methane modify the mean structure of the mesosphere and thermosphere? Geophys. Res. Lett. 16 (12), 1441–1444. http://dx.doi.org/10.1029/GL016i012p01441.

Scotto, C., Pezzopane, M., Zolesi, B., 2012. Estimating the vertical electron density profile from an ionogram: on the passage from true to virtual heights via the target function method. Radio Sci. 47, RS1007. http://dx.doi.org/10.1029/2011RS004833.

Shimazaki, T., 1955. World daily variability in the height of the maximum electron density of the ionospheric F2-layer. J. Radio Res. Lab. (Jpn.) 2, 85–97.

Smith, N., 1939. The relation of radio sky wave transmission to ionosphere measurements. Proceedings IRE 27, 332-347.

Ulich, T., Turunen, E., 1997. Evidence for long-term cooling of the upper atmosphere. Geophys. Res. Lett. 24, 1103–1106.

Upadhyay, H.O., Mahajan, K.K., 1998. Atmospheric greenhouse effect and ionospheric trends. Geophys. Res. Lett. 25, 3375–3378. http://dx.doi.org/10.1029/98GL02503.

Yiğit, E., Medvedev, A.S., 2015. Internal wave coupling processes in Earth's atmosphere. Adv. Space Res 55. http://dx.doi.org/10.1016/j.asr.2014.11.020.

Yiğit, E., Knizova, P.K., Georgieva, K., Ward, W., 2016. A review of vertical coupling in the atmosphere-ionosphere system: effects of waves, sudden stratospheric warmings, space weather, and of solar activity. J. Atmos. Sol. Terr. Phys. 141, 1–12. http://dx.doi.org/10.1016/j.jastp.2016.02.011.

Zhang, S.R., Holt, J.M., Kurdzo, J., 2011. Millstone Hill ISR observations of upper atmospheric long-term changes: height dependency. J. Geophys. Res. 116, A00H05. http://dx.doi.org/10.1029/2010JA016414.

Zhang, S.R., Holt, J.M., Erickson, P.J., Goncharenko, L.P., Nicolls, M.J., McCready, M., Kelly, J., 2016. Ionospheric ion temperature climate and upper atmospheric long-term cooling. J. Geophys. Res. Space Phys. 121. http://dx.doi.org/10.1002/2016JA022971.

Zolessi, B., Cander, L.R., 2014. Ionospheric Prediction and Forecasting. Springer-Verlag, Berlin, Germany.